JOURNAL OF ENVIRONMENTAL SCIENCES 100 (2021) 228–239

Available online at www.sciencedirect.com

ScienceDirect

www.elsevier.com/locate/jes

JES JOURNAL OF ENVIRONMENTAL SCIENCES

www.jesc.ac.cn

High pyrolysis temperature biochar reduced the transport of petroleum degradation bacteria *Corynebacterium variabile* HRJ4 in porous media

Saisai Guo[1], *Xiaomei Liu*[1,*], *Hang Zhao*[1], *Lan Wang*[1], *Jingchun Tang*[1,2,3,*]

[1] *College of Environmental Science and Engineering, Nankai University, Tianjin 300350, China.*
E-mail: 2120180637@mail.nankai.edu.cn
[2] *Key Laboratory of Pollution Processes and Environmental Criteria (Ministry of Education), Tianjin 300350, China*
[3] *Tianjin Engineering Research Center of Environmental Diagnosis and Contamination Remediation, Tianjin 300350, China*

ARTICLE INFO

Article history:
Received 24 February 2020
Revised 9 July 2020
Accepted 9 July 2020
Available online 6 August 2020

Keywords:
Gram-positive bacteria
Feedstocks
HRJ4
Transport
Retention

ABSTRACT

Biochar has been widely applied for the remediation of petroleum-contaminated soil. However, the effect of biochar on the transport of petroleum degradation bacteria has not been studied. A typical Gram-positive petroleum degradation bacteria-*Corynebacterium variabile* HRJ4 was used to study the effect of different biochars on bacterial transport and retention. Results indicated that the addition of biochar in sand was effective for reducing the transport of bacteria and poplar sawdust biochar (PSBC) had a stronger hinder effect than corn straw biochar (CSBC). The hindrance was more evident with pyrolysis temperature of biochar raised from 300°C to 600°C, which was attributed to the increase of specific surface area (309 times). The hindrance effect also enhanced with higher application rate of biochar. Furthermore, the reduction of HRJ4 transport was more obvious in higher (25 mmol/L) concentration of NaCl solution owing to electrostatic attraction enhancement. The adsorption of biochar to HRJ4 was defined to contribute to the hindrance of HRJ4 transport mainly. Combining the influence of feedstocks and pyrolysis temperature on HRJ4 transport, it suggested that specific surface area had the greatest effect on HRJ4 transport, and pore-filling, electrostatic force also contributed to HRJ4 retained in quartz sand column. At last, phenol transportation experiment indicated that the restriction of biochar on HRJ4 enhanced the phenol removal rate in the column. This study provides a theoretical basis for the interaction of biochar and bacteria, which is vital for the remediation of oil-contaminated soil and groundwater in the field.

Introduction

Soil contaminated by petroleum arising from crude oil drilling, transportation, refining, and related activities has caused great seriousness for decades (Schwab et al., 1999). Researches have demonstrated that biochar can enhance the bioremediation of petroleum-contaminated soil (Kong et al., 2018). Biochar is a carbon-rich material generated from the pyrolysis of biomass under oxygen-limited conditions (Lyu et al.,

* Corresponding author.
E-mails: liuxiaomei@nankai.edu.cn (X. Liu), tangjch@nankai.edu.cn (J. Tang).

https://doi.org/10.1016/j.jes.2020.07.012
1001-0742/

2018; Xiao et al., 2018). It has been applied in the remediation of contaminated soil due to its high porosity, cation exchange capacity, acidic functional group, a rich source of carbon and specific surface area (Saifullah et al., 2018). Many studies have confirmed that biochar can alter the community composition of indigenous microorganisms in soil by improving the nutrient availability of soil and changing soil structure and density (Kong et al., 2018; Yang et al., 2018; Yuan et al., 2019). The changes in the community composition of indigenous petroleum degradation bacteria may be relevant to bacteria transport in soil and groundwater. Therefore, when it comes to the implementation of bioremediation efforts (bioaugmentation in particular), understanding the fate and transport of petroleum bacteria in porous media is of great importance (Zhong et al., 2017).

A variety of factors may affect bacteria transport, such as the properties of biochar (Bolster and Abit, 2012; Wang et al., 2013; Suliman et al., 2017), the surface properties of bacteria (Abit et al., 2012) and liquid phase properties (Liu et al., 2017; Zhong et al., 2017; Zhao et al., 2019). In recent years, efforts have been made to study the influence of biochar amendments on the transport of bacteria in porous media (Abit et al., 2012). The effects of biochar addition on soil and soil solution properties, which had an impact on microbial transport behavior, were largely dependent on the composition and the physical and chemical properties of the biochar (Abit et al., 2012, 2014). Studies found that the properties of biochar could be affected by several factors, and the biochar feedstock and pyrolysis temperature played the most important roles (Lyu et al., 2016, 2017, 2018; Huang et al., 2017). The structure and composition of biochar determined the physical and chemical properties of biochar, including pore size distribution, pH, surface area, and surface charge. When incorporated into soils, biochar can significantly alter soil properties such as soil structure (Abit et al., 2012), soil solution pH, ionic strength and composition (Zhong et al., 2017), and the organic matter content of soil and solution, which influenced the transport of bacteria (Bolster and Abit, 2012). Concerning on surface properties of the bacteria, surface charge (Abit et al., 2012; Suliman et al., 2017), shape and size (Sasidharan et al., 2016), surface hydrophobicity (Abit et al., 2012; Suliman et al., 2017), surface macromolecular substances (Afrooz et al., 2018), chemotaxis and haptotaxis (Biria and Balouchi, 2013), physiological state and concentration (Han et al., 2013) may have influences on the transport of bacteria in porous media (Zhong et al., 2017). Abit et al. (2012) found that large differences existed during the transport procedure between the two strains of similar sizes- *E. coli*, SP2BO7 and SP1HO1, which differed in surface properties mainly depending on hydrophobicity and surface charge. This result was further confirmed by Suliman et al. (2017). Liquid phase properties such as pH (Zhao et al., 2020), temperature (Kim and Walker, 2009; Gharabaghi et al., 2015), ion (Yang et al., 2012; Balthazard-Accou et al., 2014; Gharabaghi et al., 2015) and pore-water velocity (Balthazard-Accou et al., 2014) also had a significant effect on the transport behavior of bacteria. Cations such as Na^+, K^+, Ca^{2+}, and Mg^{2+}, and anions such as Cl^-, HCO_3^-, NO_3^-, SO_4^{2-}, SiO_4^{2-} and PO_4^{3-}, are ubiquitously present in natural water systems. Many studies showed that the increase of ionic strength enhanced bacteria adsorption and inhibited the transport (Yang et al., 2012; Balthazard-Accou et al., 2014; Liu et al., 2019; Zhao et al., 2019) in the attenuation of the energy barrier for adsorption.

Up to date, comprehensive studies had analyzed the impacts of the operational conditions on bacteria transport and retention in soil or packed column. However, these researches often chose *E. coli* as the object, which belongs to Gram-negative bacteria and whose cell envelopes are composed of a thin peptidoglycan cell wall sandwiched between an inner cytoplasmic cell membrane and a bacterial outer membrane (Bolster and Abit, 2012; Han et al., 2016). On the other hand, Gram-positive bacteria have thicker cell walls with more abundant peptidoglycan and a large number of teichoic acid. The isoelectric point of Gram-positive bacteria is pH 2–3, which is lower than that of negative bacteria (pH 4–5). This means that Gram-positive bacteria would have more negative charge than Gram-negative bacteria at the same pH. To date, no study has been published on the transport and retention of Gram-positive bacteria such as some petroleum degradation bacteria in biochar-amended porous media.

Therefore, one Gram-positive bacteria - *Corynebacterium variabile* HRJ4 was chosen in this study. HRJ4 was isolated from petroleum soil sample from the Dagang Oil Field, Tianjin, China, which had been proved to be a highly efficient petroleum hydrocarbon-degrading bacterium (Zhang et al., 2016). Due to the differences in membrane composition and surface charge of Gram-positive bacteria and negative bacteria, it is important to study clearly whether and how the biochar affects the transportation of Gram-positive petroleum degrading bacteria, which is an important factor to affect the remediation of petroleum hydrocarbon contaminated soil and groundwater.

The overall objective of this work is to study the transport and retention of HRJ4 as affected by biochar in 12 cm long quartz sand column and preliminarily clarify the transport mechanism that drives the behavior of HRJ4. The specific objectives of this study were to: (1) investigate the transport and retention behavior of HRJ4 in packed quartz sand column adding biochar from different feedstocks (corn straw and poplar sawdust), two pyrolysis temperature (300 and 600°C), with three concentration (0, 1 wt.% and 5 wt.%) and at two IS (ionic strength) (10 and 25 mmol/L) NaCl solution; (2) employ single point adsorption experiment to discuss the adsorption ability of four biochar to HRJ4; (3) elucidate the mechanisms that drive/block the transport and retention behavior of HRJ4 in porous media; (4) explore the combined effects between biochar and HRJ4 on the removal rate of phenol. This paper not only provides a meaningful and comprehensive record of transport behavior of indigenous petroleum degradation bacteria HRJ4 under different conditions but also gives insight into the mechanisms governing the fate of HRJ4 in packed columns.

1. Materials and methods

1.1. *Bacteria preparation*

HRJ4 was isolated from the Dagang oil field (Tianjin, China) in our previous work (Zhang et al., 2016). The strain was cul-

tured in LB (Luria–Bertani) medium (10% sodium chloride, 10% tryptone, and 5% yeast extract powder, pH was 7.2–7.4). Firstly, HRJ4 was activated in LB medium for 12 hr at 37°C with shaking at 150 r/min in an orbital shaker (HNY-2102C, Honour, China). Then 0.1% volume of the activated medium was transferred into 100 mL LB medium and cultured to the logarithmic growth phase. After that, bacterial suspensions were centrifuged at 4000 r/min for 5 min. Cells were collected and washed three times with 0.9% NaCl. Bacterial pellets were then resuspended in 0.9% NaCl to a concentration of 10^7 CFU/mL.

SEM (scanning electron microscopy) of the bacteria: 30 mL bacterial suspensions were centrifuged at 4000 r/min for 5 min, and then cells were washed three times with 0.9% NaCl. The bacteria deposition was immobilized by 2.5% glutaraldehyde stationary solution for 2 hr and washed three times with phosphate buffer (pH 7.0). Next, cells were dehydrated with different gradient ethyl alcohol (30%, 50%, 70%, 80%, 90%, 100%), each for 15 min. Finally, the bacteria were air-dried. The structure and surface morphology of HRJ4 was characterized by SEM (JSM-7800F, JEOL, Japan).

1.2. *Porous media preparation*

The Quartz sand (ultrapure with 99.8% SiO_2) (Tianjin Jiangtian Chemical Technology Co., Ltd., China) with sizes ranging from 150 to 297 μm was used as model porous media. The sand was thoroughly cleaned priorly according to the previous method (Loveland et al., 2003). In brief, it was sonicated (100 W, 40 kHz) for 60 min, followed by immersion in sodium dithionite solution (0.1 mol/L $Na_2S_2O_4$) for 2 hr to remove surficial metallic compounds such as iron oxide and manganese oxide. Organic impurities were removed by soaking the sand in hydrogen peroxide (5% H_2O_2) for 2 hr, then washed with deionized water and subsequent for 12 hr soaking in hydrochloric acid (12 mol/L HCl). At last, the cleansed grains were washed using deionized water until pH reached 7 and dried in an oven for use.

1.3. *Biochar preparation and characterization*

Poplar sawdust and corn straw were chosen as the feedstocks of biochar. Biochar was prepared as previous studies (He et al., 2018). In brief, poplar and corn straw were crushed into small size, oven-dried at 80°C for 3 hr, and then placed in a muffle furnace (SX-G30103, Tianjin Zhonghuan electric furnace Co., Ltd., China) to produce biochar at temperatures of 300°C and 600°C for 2 hr, respectively. After that, the samples were rinsed with distilled water several times and oven-dried at 80°C. The four biochar samples were marked as PSBC300 (poplar straw biochar pyrolyzed at 300°C) and PSBC600 (poplar straw biochar pyrolyzed at 600°C), CSBC300 (corn straw biochar pyrolyzed at 300°C) and CSBC600 (corn straw biochar pyrolyzed at 600°C). The specific surface area and pore volume of the four biochar were tested by the multipoint N_2 adsorption BET (Brunauer-Emmett-Teller) method (ASAP2460, Micromeritics, America). Zeta potential of all samples was determined using a Zetasizer Nano ZS (Malvern, England). The pH value of biochar was measured using a pH meter (PB-10, Sartorius, Germany) (Rajkovich et al., 2012). The structure and surface morphology of the four biochars were characterized by SEM. The element analysis was conducted by automatic element analyzer (EA3000, Leeman, Italy).

1.4. *Column preparation*

Sterilized quartz columns (inner diameter 1.6 cm, height 15 cm) were employed as packed columns. Before packing, the biochar and quartz sand were mixed fully in a certain proportion (0, 1 wt.%, and 5 wt.% by weight) on an oscillator (HY-4A, Shanghai Lichen Instrument Technology Co., Ltd., China) at 180 r/min for two days. Then, the mixture was placed into a quartz column by vibrating the quartz column mildly. The quartz sand was packed to a height of 12 cm to prevent the generation of air bubbles in the columns and bacteria liquid outflow (Hou et al., 2017). A 200-mesh screen was laid at the end of the column to avoid the loss of quartz sand and biochar. The porosity of the packed quartz column was measured following the gravimetric method (Chen et al., 2011), with a result of about 0.41±0.03, and the PV (pore volume) was about 10 mL. The weight of quartz sand (The density of quartz sand was 2.2 g/cm^3) to fill the column to 12 cm height was 53 g. After dry-packing, the packed column was saturated and preconditioned with 10 PVs of NaCl solution (10 and 25 mmol/L) using a syringe pump (PHD ULTRA^{TM} HA3000I, Harvard Apparatus, America) at a flow rate of 5 mL/min for 20 min to establish steady hydrodynamic and chemical condition. All of the above steps were done in a sterile super-clean bench and all of the materials and solution used were sterilized in a sterilization pot (GI-54TW, Zealway Instrument Co., Ltd., America).

1.5. *Transport column experiments of HRJ4*

After column preparation, the influent was switched to HRJ4 suspension (~10^7 CFU/mL, C_0) of the same pH (7.0) and two IS (10 and 25 mmol/L). The 40 PVs of bacteria suspension was injected into the column at a flow rate of 5 mL/min by a peristaltic pump (iPump6S, Baoding Signal Fluid Technology, China) for 80 min. Followed by elution with 10 PVs of different IS (10 and 25 mmol/L) NaCl at the same flow as bacteria suspension for 20 min. Effluent samples were collected every 1 PV (2 min) by a fraction collector (BS-100A, Shanghai Jiapeng Technology Co., Ltd., China). To obtain the bacteria concentration (C) in the effluent of each microbe, a UV–spectrophotometer (T6 New Century, Persee, China) was used to analyze the turbidity at 600 nm. The pH and EC (electrical conductivity) of selected samples were also analyzed using a pH meter and conductivity meter (FE30FiveEasy, Mettler Toledo, Switzerland), respectively. After the completion of transport experiments, each column was dissected to quantify the spatial distribution of reversibly attached HRJ4 within the column. The column was excavated in 1.0 cm sections using a disposable aseptic spoon. In order to separate HRJ4 retention in the 1.0 cm quartz sand column, referring to the method of Liu et al. (2019), the 1.0 cm sections were put into 250 mL flask with 10 mL of 10 mmol/L NaOH solution and shook at 150 r/min at 30°C for 30 min. Moreover, 0.05 g/L sodium dodecylbenzene sulfonate was added, then ultrasounded for 5 min, and measured with a UV–spectrophotometer at 600 nm. The

breakthrough curves associating the relationship of C/C_0 to PV were plotted to describe the transport of HRJ4 in the saturated quartz sand. The quartz sand in the columns was replaced in every experiment, and all the experiments were carried out in triplicate. The environmental conditions were constant for all treatments investigated in the quartz sand columns.

1.6. Batch adsorption experiments

The sorption ability of different biochars to HRJ4 was assessed using single point sorption isotherms, which was referred to Abit et al. (2012) and some changes were made. Specifically, various concentration (0, 1325 and 6625 mg/L) of biochars, which was equal to the biochar concentration (0, 1 wt.% and 5 wt.%) in the column and 100 mL of two IS (10 and 25 mmol/L) NaCl solutions were added to a 250 mL flask. Then, 10 mL bacterial solution centrifugated at 4000 r/min for 5 min (equivalent to ~10^8 CFU/mL) were prepared as described in the bacterial preparation and added in the flask to start adsorption experiment. As a result, the concentration of bacteria in the flask was 10^7 CFU/mL (C_0). The time of adsorption lasted for 80 min to keep pace with the time of bacteria transport in the quartz sand column. After adsorption, the above mixture was then centrifuged at 25°C at 1200 r/min for 5 min, and 3 mL of the supernatant was extracted and quantified (C') using a UV– spectrophotometer at 600 nm. Finally, C'/C_0 was calculated and all of the sorption experiments were conducted in triplicate.

After batch adsorption, a small part of a mixture of biochar and HRJ4 was put into a 2 mL plastic centrifuge tube. The SEM detecting procedure followed as mentioned above in "SEM of the bacteria."

After batch adsorption, 100 μL mixture was put into a 500 μL centrifuge tube, mixed with 100 μL PI (Propidium Iodide) and SYBR Green (V: V = 1:1 mixture). Then, the sample was incubated on a shaker at 30°C for 15 min in the dark. At last, CLSM (Confocal laser scanning microscope) (LSM880 with Airyscan, Zeiss, Germany) was used with green (excitation 485 nm and emission 530 nm) and red (excitation 485 nm and emission 630 nm) fluorescence wavelengths to distinguish the living and dead HRJ4 bacteria as well as to characterize it presence state on biochar surface with 40 × objective lens. Every sample was dyed with PI and SYBR Green.

1.7. Column transport experiments of phenol and bacteria

The column was prepared as mentioned above "column preparation", 40 PVs of bacteria suspension (~10^7 CFU/mL) was injected into the column at a flow rate of 0.5 mL/min by a peristaltic pump (iPump6S, Baoding signal fluid technology, China) for 80 min, marked as HRJ4, and control' group was conducted by 25 mmol/L NaCl solution, then 80 PVs of 50 mg/L phenol solution (C_0') was injected at the same flow as bacteria suspension for 400 min. The sample was collected from every other PV and put into the refrigerator immediately to eliminate the influence caused by further degradation of microorganisms. The concentration of phenol was tested according to water quality analysis method (HJ 503–2009, China).

1.8. Data analysis

One-way analysis of variance (ANOVA) was performed to identify statistically significant differences in measured parameters. The mean removal efficiencies were separated by Tukey's honestly significant difference (HSD) test ($P < 0.05$). All statistical analyzes were performed using IBM SPSS Statistics for Windows Version 22.0.

2. Result and discussion

2.1. Biochar properties and characterization

In order to analyze the reasons of different raw materials (corn straw and poplar sawdust) on HRJ4 transport in quartz sand column, the physicochemical properties (e.g., pH, specific surface area, average pore diameter, element analysis) of these biochars which may affect the bacteria transport were characterized in Table 1 and the morphology of biochar was presented in Fig. 1**a-d**. As exhibited in Fig. 1, the surface of PSBC (poplar straw biochar) (**a** and **b**) was rougher than that of CSBC (corn straw biochar) (**c** and **d**). The pore of PSBC was round (Fig. 1**a, b**), and that of CSBC was oval and smaller (Fig. 1**c, d**). Specifically, the pH value of CSBC was higher than that of PSBC and the pH value enhanced with the increase of pyrolysis temperature (Table 1), and the content of N, H, O, and ash content of CSBC was higher than that of PSBC, only C content was opposite, which was consistent with Tryon et al. (1948). Moreover, the pH value of all those biochars used in this study were > 7, indicating that the four biochars presented alkalinity. Besides, Huang et al. (2017) and Lyu et al. (2019) discovered that the ζ-potential of biochar was negative and it would decrease with pH raised from 3 to 9 in general. In this study, the same finding was shown in Fig. 2.

2.2. Effects of biochar feedstocks, pyrolysis temperature, concentration, and NaCl solution is on HRJ4 transport in the packed column

Two feedstock biochar had a significant difference in peak C/C_0 (Fig. 3**a-d**) and fractional recovery (fr) values (Table 2) at two IS NaCl solution. For the same IS NaCl solution, fr in PSBC was lower than that in CSBC (Table 2). For example, when biochar concentration was 5 wt.%, fr value of PSBC600 was almost 1.5 and 2.5 folds higher than that of CSBC600 at 10 mmol/L and 25 mmol/L NaCl solution, respectively. Moreover, the equilibrium values of the breakthrough curve of CSBC (Fig. 3**a-d**) were higher than that of PSBC (Fig. 3**a-d**), which indicated that PSBC had more resistant effect on bacteria transport in the quartz sand column. It can be found that ζ-potentials of HRJ4 in NaCl solution were also negative (Table 3). Thus, the interaction force between biochar and bacteria in this study was a repulsive force. That was to say, the repulsive force between PSBC and HRJ4 was slighter than that between CSBC and HRJ4 as shown from the higher zeta potential values in PSBC, so HRJ4 was easier to attach to PSBC, and this also explained why PSBC had a greater hindrance on HRJ4 than CSBC.

For biochar from different pyrolysis temperatures - BC300 (PSBC300 and CSBC300) and BC600 (PSBC600 and CSBC600),

Table 1 – Characteristics of biochar particles from different raw materials (corn straw and poplar sawdust) and pyrolysis temperature (300 and 600 °C).

	CSBC		PSBC	
	300°C	600°C	300°C	600°C
Average pore diameter (nm)	11.99	1.78	10.01	1.70
Specific surface area (m^2/g)	1.06 ± 0.01	328.10±2.05	1.01 ± 0.01	364.55±2.75
Micropore volume (cm^3/g)	0.0002	0.1083	0.0001	0.1205
Total pore volume (cm^3/g)	0.0032	0.1463	0.0025	0.1555
pH	7.58±0.01	8.85±0.03	7.24±0.02	7.98±0.02
C (%)	63.13±0.20	66.26±0.21	68.40±0.42	74.70±0.34
N (%)	1.42±0.11	1.33±0.00	1.32±0.13	1.17±0.13
H (%)	5.29±0.26	4.699±0.08	2.02±0.02	1.65±0.02
O (%)	19.50±0.05	13.19±0.29	19.36±0.28	10.48±0.23
Ash (%)	11.56±0.13	12.93±0.06	9.90±0.10	10.99±0.05
H/C (%)	0.084	0.071	0.030	0.022
O/C (%)	0.309	0.199	0.283	0.140
(O + N)/C (%)	0.331	0.219	0.302	0.156

CSBC: corn straw biochar; PSBC: poplar straw biochar.

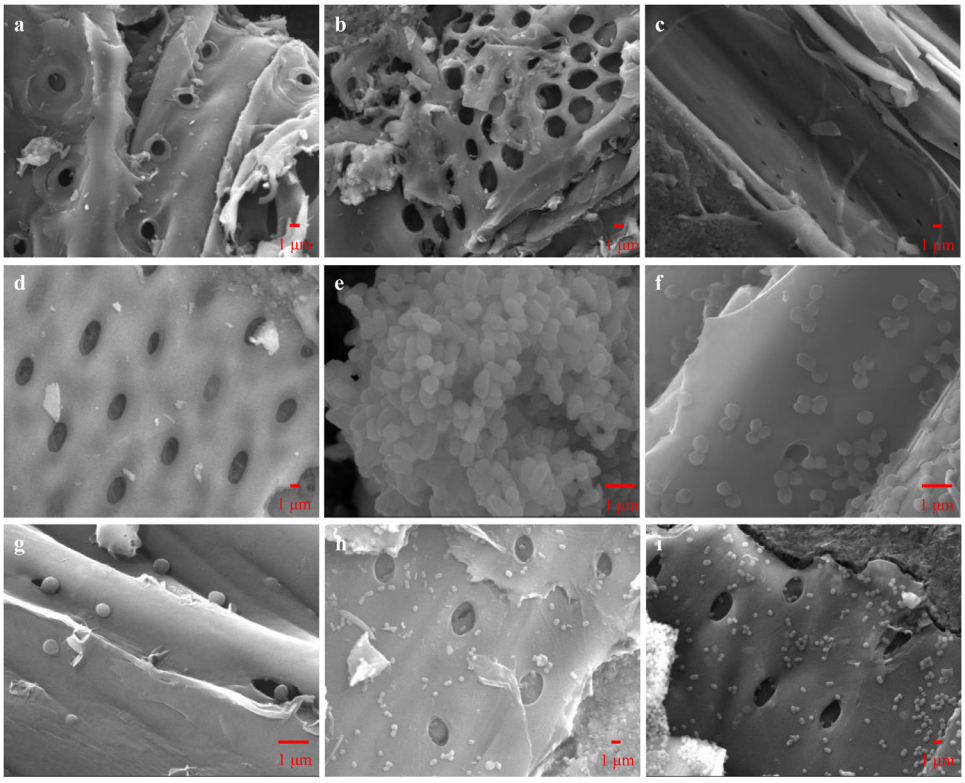

Fig. 1 – SEM images of PSBC300 (a), PSBC600 (b), CSBC300 (c), CSBC600 × 3000 times (d); SEM images of HRJ4 (e), PSBC300 and HRJ4 × 10,000 times (f), CSBC300 and HRJ4 × 10,000 times (g), PSBC600 and HRJ4 × 3000 times (h), CSBC600 and HRJ4 × 3000 times (i). PSBC300 and PSBC600: poplar straw biochar pyrolyzed at 300°C and 600°C respectively; CSBC300 and CSBC600: corn straw biochar pyrolyzed at 300°C and 600°C respectively.

the transport and retention behavior of the bacteria were diverse. For instance, in 10 mmol/L NaCl solutions, no matter what the biochar concentration was, fr value of BC300 was about 2–2.5 folds higher than that of BC600. The distinction was more obvious in 25 mmol/L NaCl solution, after adding 1 wt.% biochar, fr value of BC300 was 2.75–6.3 folds of BC600. The most significant difference originated from temperature variation appeared under 5 wt.% biochar addition in 25 mmol/L NaCl solution, fr value of BC300 was 4–6.8 folds of BC600 (Table 2). Also, with regard to the breakthrough curve, the peak C/C_0 of BC300 was higher than that of BC600 in all treatments. Besides, BC300 reached equilibrium within a shorter time as compared to that of BC600. All of the results implied that low-temperature biochar (BC300) had a

Table 2 – Percent of *Corynebacterium variabile* HRJ4 received in Effluent (fr), percentage of HRJ4 extracted (Ex) from quartz sand column dissections, and the ratio of bacteria that were unaccounted for and assumed to be unextractable (UEx) from quartz sand column dissections*.

	Quartz sand	CSBC				PSBC			
		300°C		600°C		300°C		600°C	
	0	1 wt.%	5 wt.%	1 wt.%	5 wt.%	1 wt.%	5 wt.%	1 wt.%	5 wt.%
fr	51.36a	49.12a	46.26a	28.68a	22.35d	39.34b	31.79c	16.26de	14.29e
Ex	28.82ef	22.18f	26.32f	40.18d	56.89bc	34.12e	52.98c	59.82b	71.24a
UEx	19.82bc	22.7b	27.42ab	31.14a	20.76bc	26.54ab	15.23c	23.92ab	14.47c
fr	48.36a	42.31a	40.96a	24.19b	10.07d	19.76c	26.86b	3.13e	3.94e
Ex	36.82e	32.49e	34.69e	60.61c	76.65b	48.30d	58.13c	85.76a	86.17a
UEx	14.82c	25.20b	24.35b	15.20c	13.28cd	31.94a	15.01c	11.11cd	9.89d

* Mean values in each row followed by the same lowercase letters are not significantly different using Tukey's Honestly Significant Difference test at $p < 0.05$.

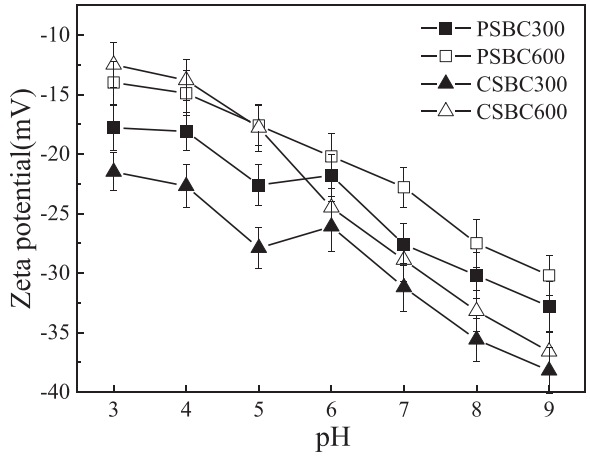

Fig. 2 – Zeta potential of PSBC pyrolyzed at 300°C (PSBC300) and 600°C (PSBC600) as well as CSBC pyrolyzed at 300°C (CSBC300) and 600°C (CSBC600) under pH value from 3 to 9.

lighter hindrance on the transport behavior of HRJ4 than high-temperature biochar (BC600).

To test whether biochar concentration can impact HRJ4 transport, HRJ4 transportation in packed column after adding 0, 1 wt.% and 5 wt.% biochar was investigated. From fr value of effluent (Table 2), there was a negative correlation between fr value and biochar concentration, which meant that the retention effect of biochar decreased with the increase of biochar concentration. As shown in Fig. 3, compared with the control without biochar (star), breakthrough curves of the other treatments reached the plateau faster. Moreover, the C/C_0 of breakthrough plateau decreased with the increase of biochar concentration. For instance, under all treatments, when the breakthrough curve reached equilibrium, the C/C_0 of control without biochar was 0.7–0.8, while C/C_0 decreased to 0.5–0.6 after adding 1 wt.% biochar. When the concentration of biochar was 5 wt.%, C/C_0 was only 0.3–0.5. These results suggested that for four biochar samples, HRJ4 transport in the packed column was dependent on biochar concentration. In other words, biochar particle had a hindrance effect to the HRJ4 transport in the quartz sand column, and the hindrance enhanced with the increase of biochar concentration (Sasidharan et al., 2016; Suliman et al., 2017).

The transport behavior of HRJ4 in packed quartz sand column was examined at two IS (10 mmol/L and 25 mmol/L NaCl solution). As shown in Table 2, IS of NaCl solution used in this experiment had a great impact on transport behavior. For HRJ4, fr was always lower in 25 mmol/L NaCl solution than that in corresponding 10 mmol/L NaCl solution. Hence, when the IS of NaCl solution was increased, the effluent percentages of HRJ4 was reduced. Furthermore, the breakthrough plateaus at high IS (25 mmol/L) (Fig. 3**a, b**) were lower than those at low IS (10 mmol/L) (Fig. 3**c, d**) under all treatments.

2.3. *Characterization on retained profiles in different position of the column*

When the transport experiment finished, the quartz sand column retained bacteria were dug to study the distribution of bacteria in the column. The percentage of HRJ4 extracted from quartz sand column dissections (Ex) was exhibited in Table 2. The retained curve in NaCl (10 and 25 mmol/L) with (1 wt.% and 5 wt.% of different raw material and pyrolysis temperature biochar) or without biochar were shown in Fig. 4. The bacteria retained in quartz sand column without biochar particles were less than those adding biochar particles under both IS NaCl solutions. Specifically, log(bacteria) raised with the biochar concentration increased, which indicated that more bacteria were blocked in the quartz sand column. The above results indicated that the existence of biochar particles enhanced the retaining of HRJ4 in the quartz sand column in NaCl solution (10 and 25 mmol/L).

Further inspection observed that the amount of HRJ4 varied from the distances in the quartz sand column with or without biochar particles (Fig. 4). It illustrated that because of the existence of biochar particles, the increased retention of bacteria in solutions mainly appeared at the segments near the column inlet, which was 0.5 cm to the top surface of the quartz sand column, and this was consistent with previous studies (Suliman et al., 2017). Since HRJ4 can attach to biochar particles, it would form biochar-HRJ4 clusters, and the clusters

Table 3 – Zeta potential (mV) and conductivity of quartz sand, HRJ4 and biochar in NaCl solution (10 and 25 mmol/L) at pH 7.

Sample	Pyrolysis temperature (°C)	Ionic strength (mmol/L)	Zeta potential (mV)	Conductivity (mS/cm)
Quartz sand	–	10	−49.6 ± 0.84	1.52±0.56
	–	25	−47.0 ± 0.36	3.49±0.78
HRJ4	–	10	−36.8 ± 0.56	1.31±0.80
	–	25	−34.4 ± 0.54	3.56±0.94
CSBC+HRJ4	300	10	−36.4 ± 0.97	1.38±0.95
		25	−35.2 ± 1.21	2.9 ± 0.91
	600	10	−39.8 ± 0.98	1.34±0.89
		25	−40±0.73	3.25±0.85
PSBC+HRJ4	300	10	−38.5 ± 0.81	1.33±0.81
		25	−39.8 ± 0.92	3.32±0.88
	600	10	−37.4 ± 0.78	1.36±0.78
		25	−36.3 ± 0.83	3.31±0.76
Quartz sand+ CSBC+HRJ4	300	10	−39.9 ± 0.59	1.3 ± 0.68
		25	−33.7 ± 0.72	2.86±0.69
	600	10	−37.8 ± 0.69	1.27±0.83
		25	−36±0.91	3.42±0.69
Quartz sand+PSBC+HRJ4	300	10	−41.3 ± 0.82	1.37±0.68
		25	−34.2 ± 0.97	3.33±0.87
	600	10	−39.8 ± 0.78	1.31±0.73
		25	−38.6 ± 0.93	3.29±0.74

CSBC+HRJ4: treatment of corn straw biochar and HRJ4; PSBC+HRJ4: treatment of poplar straw biochar and HRJ4; Quartz sand+ CSBC+HRJ4: treatment of Quartz sand, corn straw biochar and HRJ4; Quartz sand+PSBC+HRJ4: treatment of Quartz sand, poplar straw biochar and HRJ4.

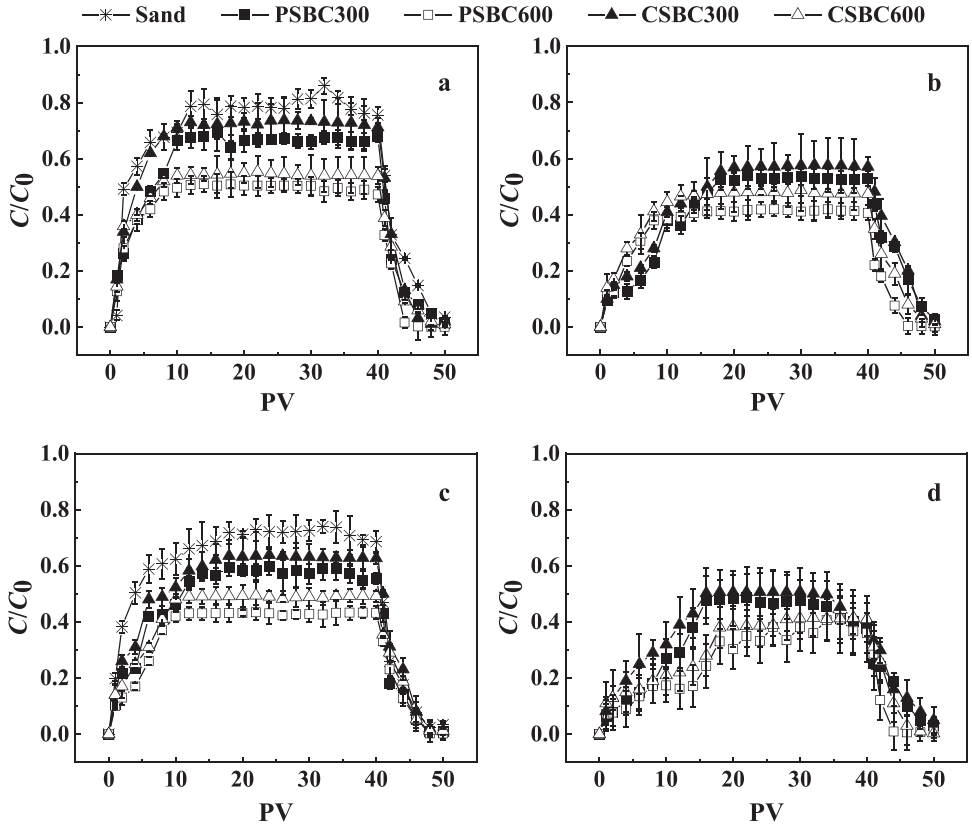

Fig. 3 – Breakthrough curves for HRJ4 at 10 mmol/L (a, b) NaCl solution and 25 mmol/L (c, d) with the PSBC and CSBC and 300°C and 600°C of 1 wt.% (a, c) and 5 wt.% (b, d) biochar. Star represents the control that is without biochar. Error bars represent the range of two replicate experiments ($n = 3$). PV: pore volume.

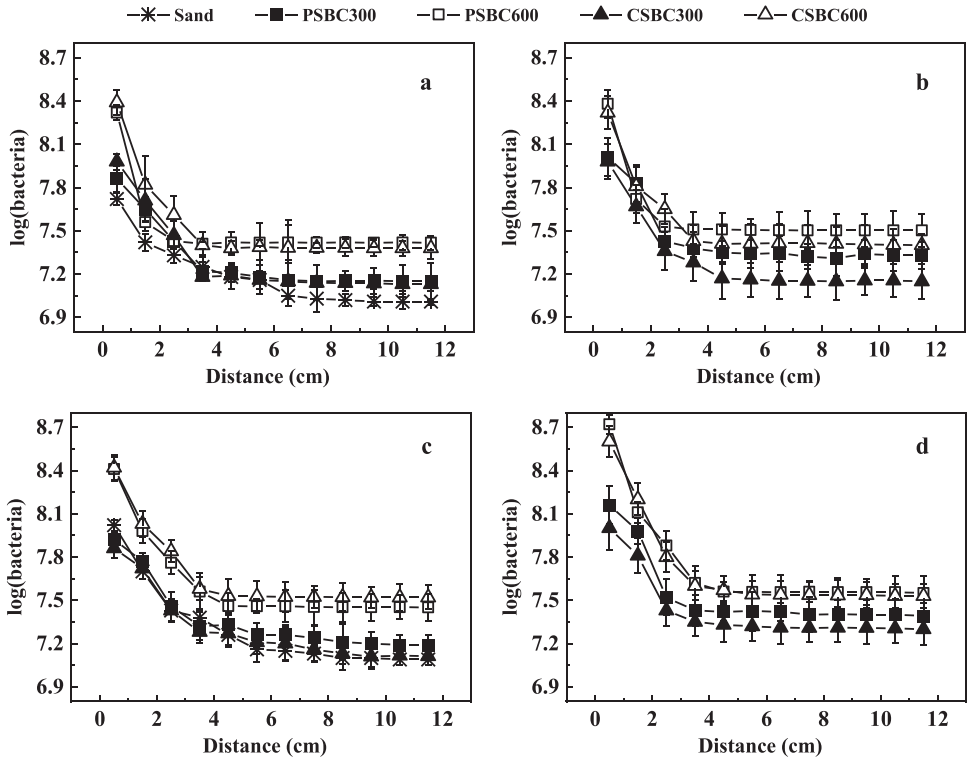

Fig. 4 – Retained profiles in quartz sand column for HRJ4 at 10 mmol/L (a, b) NaCl solution and 25 mmol/L (c, d) NaCl solution with the PSBC and CSBC and 300°C and 600°C of 1 wt.% (a, c) and 5 wt.% (b, d) biochar. Star represent control without biochar. Error bars represented the standard deviations in triplicate transport experiments.

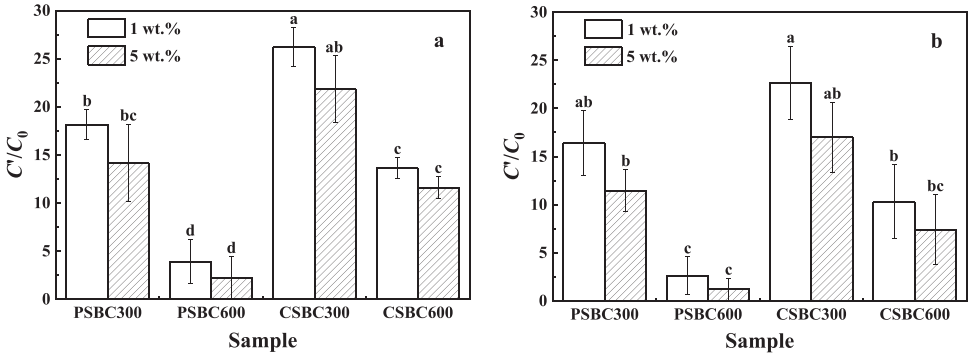

Fig. 5 – Results of C'/C0 (C' is the amount of HRJ4 in effluent after batch experiment. C0 is˜107 CFU/mL, C0 is initial bacterial concentration in solution) after batch adsorption experiment under 10 mmol/L (a) and 25 mmol/L (b) NaCl solution. Blank represents biochar concentration is 1 wt.%, slant represents biochar concentration is 5 wt.%. The same letters above the bars indicate no significant differences between groups according to ANOVA at P level of 0.05.

would grow more prominent over time, especially at column inlet. The number of the retained bacteria in the column decreased with the increase of the distance to the top surface of the column under all conditions. When the distance to the top surface was or exceeded to 4.5 cm, the number of retained bacteria did not change dramatically.

2.4. *Batch adsorption experiments*

Batch experiments were conducted to examine the adsorption property between biochar and HRJ4. Fig. 5 showed the normalized bacterium concentrations in equilibrated solutions (C'/C_0: C_0 is the initial concentration and C' is the final concentration) after 80 min mixing in flasks containing various types of biochars in NaCl solution (10 and 25 mmol/L). Control flasks (without biochar and sand) confirmed stable bacteria concentration (no loss due to inactivation or attachment to tube wall) during the course of experiments (data not shown). It was observed that C'/C_0 after treated with high-temperature biochar (BC600, biochar pyrolyzed at 600°C including PSBC300 and CSBC300) was significantly lower than that of low-temperature biochar (BC300, biochar pyrolyzed at

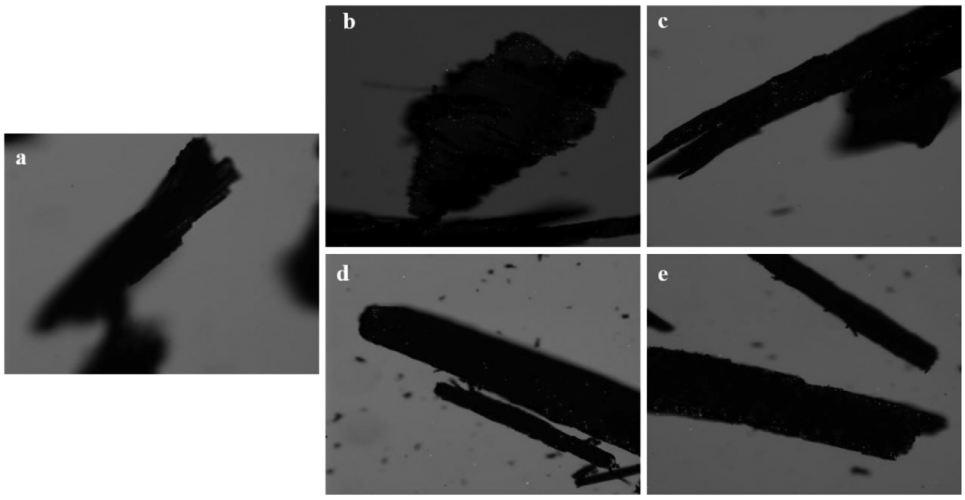

Fig. 6 – Microscopic images of microspheres (bright fluorescent spheres) attached to biochar after batch experiments, objective amplification was 40 × . (a) is control (without bacteria) and (b-e) is test group (with bacteria) under 25 mmol/L NaCl. b, c, d and e is CSBC300, CSBC600, PSBC300 and PSBC600, respectively.

300°C including PSBC600 and CSBC600). These results clearly demonstrated that the tendency of bacteria HRJ4 adsorption to high-temperature biochar was stronger.

Sorption is a surface phenomenon and depends on the specific surface area to a large extent. The specific reasons for the above results in the batch experiments weren't explained clearly in the previous study (Mohanty et al., 2014). Abit et al. (2012) used the pyrolysis temperature range similar to this study and found that as the increase of pyrolysis temperature, there were greater hydrophobic attractions between bacteria and biochar, because of the increased microporosity of biochars and higher specific surface areas with higher adsorption potential to the bacterial outer membrane. In this study, it indicated that the specific surface area increased sharply with the increase of pyrolysis temperature from 300 to 600°C. Simultaneously, the biochar pyrolyzed at high temperatures exposed more holes and ravines, which was conducive to the attachment of bacteria. This may explain why high-temperature biochar had a stronger attachment to HRJ4 than low-temperature biochar.

Fig. 6 was the CLSM images of bacteria HRJ4 and biochar after batch experiments. The results confirmed the attachment of the bacteria to the surfaces of the biochar. However, it could provide only qualitative analysis, not quantitative analysis. Besides, there was hardly any red fluorescence, which meant during the batch adsorption experiment, there was no significant change in bacterial survival rate. As the condition of HRJ4 transport in the packed column was almost the same as that of batch adsorption experiment, there was no apparent cell death during the experiment, which meant that the hindrance of biochar and NaCl solution had nothing to do with bacterial death.

To explain the relation between bacteria and petroleum-polluted soil, the simultaneous transportation of phenol and bacteria in quartz column experiment was conducted with 5% PSBC600 which had the most excellent ability to hinder the HRJ4 transport in the column. Phenol is an important component of petroleum, so we selected it as a typical pollutant to do experiments. As shown in Fig. 7, the phenol migration rate with HRJ4 was lower than that of the control', so that the penetration time was delayed. After the transport experiment, the phenol concentration of the treatment of PSBC600 was lower than that of control'. This phenomenon confirmed that the hindrance effect of biochar on HRJ4 increased the removal rate of phenol in the quartz sand column, which enhanced the contact time among biochar, HRJ4, and phenol (Zhao et al., 2020). The adsorption of biochar on phenol and HRJ4 provided longer time for HRJ4 to degrade phenol.

2.5. *Relation between different factors and mechanism analysis*

From what has been discussed above, we found that PSBC, higher pyrolysis temperature, biochar concentration, and solution IS reduced the transport of HRJ4 in the quartz sand column. Several factors may account for this phenomenon. The first factor was the biochar structure—the different surface roughness of biochar. Aller (2016) showed that feedstock had an impact on biochar structure. In addition to the surface roughness of biochar, Abit et al. (2012) had proposed that pore structure might affect bacteria transport and retention in porous media. Judging from the consequence of this study (Fig. 1), HRJ4 may be more likely to get on the biochar of round pore. Of course, more investigations are needed to determine whether surface roughness or biochar pore shape was the main factor that affected the adsorption capacity of bacteria. Moreover, Lehmann et al. (2011) had proved that the internal surfaces of biochar might lead to additional attachment sites and more effective entrapment of colloids. Based on internal pore diameter, the pore can be classified into three types, macropores (> 50 nm), mesopores (2–50 nm), and micropores (< 2 nm). Previous research (Aller, 2016) has concluded that macropores are responsible for high adsorptive capacities of bacteria. Fig. 1**a-d** showed that BC600 had more macropores than BC300 on the surface. Also, the macropores diameter of BC300 was 1.5–2.5 μm (Fig. 1**a, c**), while that of BC600 were

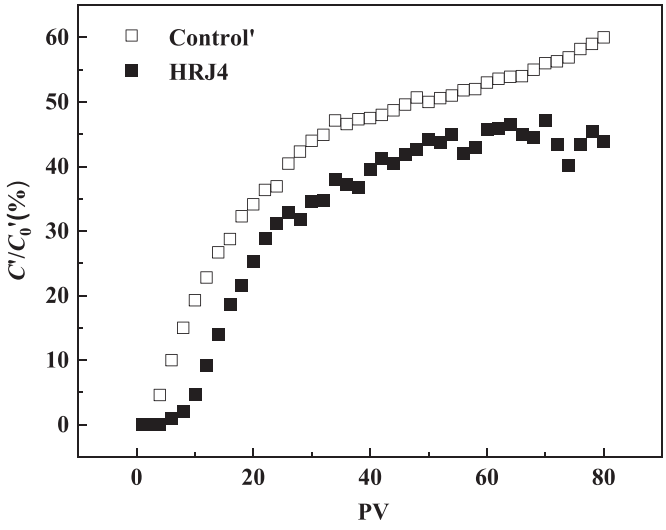

Fig. 7 – The breakthrough curve of phenol in bacterial HRJ4-enhanced biochar. Control' meant phenol transport in the column packed with PSBC600, but there were no HRJ4. HRJ4 treatment meant phenol transport in the column packed with PSBC600 and HRJ4.

4–6 μm (Fig. 1b, d), HRJ4 was 0.8–1.2 μm Fig. 1e, which was smaller than the diameter of macropore. That meant all or part of HRJ4 was very likely to be trapped into the macropore of biochar and there was no doubt that bacteria was much easier to be entrapped into larger pores of biochar. This was consistent with the results of fr value. Therefore, the pore-filling mechanism of biochar may be employed to account for this phenomenon. Besides, biochar pyrolyzed at high temperatures (600°C) had a more specific surface area. Previous studies (Bolster and Abit, 2012; Wang et al., 2013; Suliman et al., 2016) have obtained the same conclusion, indicating that the effects of pyrolysis temperature on bacteria transportation mainly depended on the specific surface areas. And the reason for surface area difference may be attributed to pore size distribution.

Furthermore, previous studies (Song and Guo, 2012; Zhao et al., 2013; Xiao et al., 2018) had stated that the pH of biochar pyrolyzed at high temperature was high, so was in this study. In Table 3, the ζ-potential of BC600 was more negatively charged than that of BC300. However, the ζ-potential difference originated from pyrolysis temperature was not significant. Thus, the electrostatic force was not the main reason for the effect of biochar pyrolysis temperature on HRJ4 transport in the quartz sand column. In addition, it can be concluded that IS in packed columns was proportional to the hindrance degree of HRJ4 transport. This can be explained by less negative ζ potential at high IS and more conductivity at high IS (Table 3), so the repulsive electrostatic interactions among them was attenuated according to classic DLVO (Derjaguin-Landau-Verwey-Overbeek) theory (Rijnaarts et al., 1999), which was also showed in previous studies (Yang et al., 2012; Balthazard-Accou et al., 2014).

To sum up, biochar (from two feedstocks and pyrolysis temperature) enhanced the retention of petroleum degradation bacteria HRJ4 in the quartz sand column experiment. The adsorption of biochar to HRJ4 was mainly contributed to the hindrance of HRJ4 transport in a packed column. Considering the influence of feedstocks and pyrolysis temperature on HRJ4 transport, specific surface areas had the greatest effect on HRJ4 transport efficiency. Whereas, in addition to surface adsorption, the pore-filling also existed in the retention of HRJ4 in the column, which means pore size and structure will influence HRJ4 transport. Last but not least, electrostatic interactions also contributed to HRJ4 retention in the quartz sand column in that the increase in IS resulted in more negatively charged in the effluent.

3. Conclusions

In this study, a typical Gram-positive petroleum degradation bacteria HRJ4 was used to analyze the transport and retention behavior of bacteria in 12 cm long quartz sand column. Results suggested that biochar was effective for reducing bacterial transport through quartz sand column and the effect depended on the feedstock, pyrolysis temperature and concentration of biochar as well as IS of NaCl solution. Compared with CSBC, PSBC had a greater hindrance on HRJ4 transport. The retained degree of HRJ4 transport in quartz sand column increased with the pyrolysis temperature and concentration of biochar as well as IS. The main mechanism between the transport of HRJ4 in quartz sand column was surface absorption. In addition, biochar could restrict phenol transport in quartz sand, so the degradation rate of phenol by HRJ4 was increased. This study provided a theoretical basis for the combined application of biochar and petroleum hydrocarbon-degrading bacteria in petroleum-polluted soil.

Acknowledgments

This work was supported by the National Natural Science Foundation of China (Nos. U1806216, 41877372) and the 111 program, Ministry of Education, China (No. T2017002).

REFERENCES

Abit, S.M., Bolster, C.H., Cai, P., Walker, S.L., 2012. Influence of feedstock and pyrolysis temperature of biochar amendments on transport of *Escherichia coli* in saturated and unsaturated soil.. Environ. Sci. Technol. 46 (15), 8097–8105.

Abit, S.M., Bolster, C.H., Cantrell, K.B., Flores, J.Q., Walker, S.L., 2014. Transport of *Escherichia coli*, *Salmonella typhimurium*, and microspheres in biochar-amended soils with different textures.. J. Environ. Qual. 43 (1), 371–378.

Afrooz, A.R.M.N., Pitol, A.K., Kitt, D., Boehm, A.B., 2018. Role of microbial cell properties on bacterial pathogen and coliphage removal in biochar-modified stormwater biofilters. Environ. Sci.-Wat. Res. Technol. 4 (12), 2160–2169.

Aller, M.F., 2016. Biochar properties: transport, fate, and impact. Crit. Rev. Environ. Sci. Technol. 46 (14–15), 1183–1296.

Balthazard-Accou, K., Fifi, U., Agnamey, P., Casimir, J.A., Brasseur, P., Emmanuel, E., 2014. Influence of ionic strength and soil characteristics on the behavior of *Cryptosporidium* oocysts in saturated porous media. Chemosphere. 103, 114–120.

Biria, D., Balouchi, A., 2013. Investigation of the role of chemotaxis in bacterial transport through saturated porous media using Taguchi approach. Colloid Surf. A-Physicochem. Eng. Asp. 436, 542–548.

Bolster, C.H., Abit, S.M., 2012. Biochar pyrolyzed at two temperatures affects transport through a sandy soil. J. Environ. Qual. 41 (1), 124–133.

Chen, G., Liu, X., Su, C., 2011. Transport and retention of TiO_2 rutile nanoparticles in saturated porous media under low-ionic-strength conditions: measurements and mechanisms. Langmuir. 27 (9), 5393–5402.

Gharabaghi, B., Safadoust, A., Mahboubi, A.A., Mosaddeghi, M.R., Unc, A., Ahrens, B., et al., 2015. Temperature effect on the transport of bromide and E. coli NAR in saturated soils.. J. Hydrol. 522, 418–427.

Han, Y., Hwang, G., Kim, D., Bradford, S.A., Lee, B., Eom, I., et al., 2016. Transport, retention, and long-term release behavior of ZnO nanoparticle aggregates in saturated quartz sand: role of solution pH and biofilm coating. Water Res. 90, 247–257.

Han, P., Shen, X., Yang, H., Kim, H., Tong, M., 2013. Influence of nutrient conditions on the transport of bacteria in saturated porous media. Colloid Surf. B-Biointerfaces. 102, 752–758.

He, R., Peng, Z., Lyu, H., Huang, H., Nan, Q., Tang, J., 2018. Synthesis and characterization of an iron-impregnated biochar for aqueous arsenic removal. Sci. Total Environ. 612, 1177–1186.

Hou, J., Zhang, M., Wang, P., Wang, C., Miao, L., Xu, Y., et al., 2017. Transport, retention, and long-term release behavior of polymer-coated silver nanoparticles in saturated quartz sand: the impact of natural organic matters and electrolyte. Environ. Pollut. 229, 49–59.

Huang, Y., Tang, J., Gai, L., Gong, Y., Guan, H., He, R., et al., 2017. Different approaches for preparing a novel thiol-functionalized graphene oxide/Fe-Mn and its application for aqueous methylmercury removal. Chem. Eng. J. 319, 229–239.

Kim, H.N., Walker, S.L., 2009. *Escherichia coli* transport in porous media: influence of cell strain, solution chemistry, and temperature.. Colloid Surf. B-Biointerfaces. 71 (1), 160–167.

Kong, L., Gao, Y., Zhou, Q., Zhao, X., Sun, Z., 2018. Biochar accelerates PAHs biodegradation in petroleum-polluted soil by biostimulation strategy. J. Hazard. Mater. 343, 276–284.

Lehmann, J., Rillig, M.C., Thies, J., Masiello, C.A., Hockaday, W.C., Crowley, D., 2011. Biochar effects on soil biota-A review. Soil. Biol. Biochem. 43 (9), 1812–1836.

Liu, Z., Han, Y., Jing, M., Chen, J., 2017. Sorption and transport of sulfonamides in soils amended with wheat straw-derived biochar: effects of water pH, coexistence copper ion, and dissolved organic matter. J. Soil. Sediment. 17 (3), 771–779.

Liu, L., Liu, G., Zhou, J., Wang, J., Jin, R., 2019. Cotransport of biochar and *Shewanella oneidensis* MR-1 in saturated porous media: impacts of electrostatic interaction, extracellular electron transfer and microbial taxis. Sci. Total Environ. 658, 95–104.

Loveland, J.P., Bhattacharjee, S., Ryan, J.N., Elimelech, M., 2003. Colloid transport in a geochemically heterogeneous porous medium: aquifer tank experiment and modeling. J. Contam. Hydrol. 65 (3–4), 161–182.

Lyu, H., He, Y., Tang, J., Hecker, M., Liu, Q., Jones, P.D., et al., 2016. Effect of pyrolysis temperature on potential toxicity of biochar if applied to the environment. Environ. Pollut. 218, 1–7.

Lyu, H., Tang, J., Huang, Y., Gai, L., Zeng, E.Y., Liber, K., et al., 2017. Removal of hexavalent chromium from aqueous solutions by a novel biochar supported nanoscale iron sulfide composite. Chem. Eng. J. 322, 516–524.

Lyu, H., Xia, S., Tang, J., Zhang, Y., Gao, B., Shen, B., 2019. Thiol-modified biochar synthesized by a facile ball-milling method for enhanced sorption of inorganic Hg^{2+} and organic CH_3Hg^+. J. Hazard. Mater. 384, 121357–121367.

Lyu, H., Zhao, H., Tang, J., Gong, Y., Huang, Y., Wu, Q., et al., 2018. Immobilization of hexavalent chromium in contaminated soils using biochar supported nanoscale iron sulfide composite. Chemosphere. 194, 360–369.

Mohanty, S.K., Cantrell, K.B., Nelson, K.L., Boehm, A.B., 2014. Efficacy of biochar to remove *Escherichia coli* from stormwater under steady and intermittent flow. Water Res. 61, 288–296.

Rajkovich, S., Enders, A., Hanley, K., Hyland, C., Zimmerman, A.R., Lehmann, J., 2012. Corn growth and nitrogen nutrition after additions of biochars with varying properties to a temperate soil. Biol. Fertil. Soils. 48 (3), 271–284.

Rijnaarts, H.H.M., Norde, W., Lyklema, J., Zehnder, A.J.B., 1999. DLVO and steric contributions to bacterial deposition in media of different ionic strengths. Colloid Surf. B-Biointerfaces. 14 (1–4), 179–195.

Saifullah, Dahlawi, S., Naeem, A., Rengel, Z., Naidu, R., 2018. Biochar application for the remediation of salt-affected soils: challenges and opportunities. Sci. Total Environ. 625, 320–335.

Sasidharan, S., Torkzaban, S., Bradford, S.A., Kookana, R., Page, D., Cook, P.G., 2016. Transport and retention of bacteria and viruses in biochar-amended sand. Sci. Total Environ. 548-549, 100–109.

Schwab, A.P., Su, J., Wetzel, S., Pekarek, S., Banks, M.K., 1999. Extraction of petroleum hydrocarbons from soil by mechanical shaking. Environ. Sci. Technol. 33 (11), 1940–1945.

Song, W., Guo, M., 2012. Quality variations of poultry litter biochar generated at different pyrolysis temperatures. J. Anal. Appl. Pyrolysis. 94, 138–145.

Suliman, W., Harsh, J.B., Abu-Lail, N.I., Fortuna, A., Dallmeyer, I., Garcia-Perez, M., 2016. Influence of feedstock source and pyrolysis temperature on biochar bulk and surface properties. Bioresour. Technol. 84, 37–48.

Suliman, W., Harsh, J.B., Fortuna, A., Garcia-Pérez, M., Abu-Lail, N.I., 2017. Quantitative effects of biochar oxidation and pyrolysis temperature on the transport of pathogenic and nonpathogenic *Escherichia coli* in biochar-amended sand columns.. Environ. Sci. Technol. 51 (9), 5071–5081.

Tryon, E.H., 1948. Effect of charcoal on certain physical, chemical, and biological properties of forest soils. Ecol. Monogr. 18 (1), 81–115.

Wang, D., Zhang, W., Hao, X., Zhou, D., 2013. Transport of biochar particles in saturated granular media: effects of pyrolysis temperature and particle size. Environ. Sci. Technol. 47 (2), 821–828.

Xiao, X., Chen, B., Chen, Z., Zhu, L., Schnoor, J.L., 2018. Insight into multiple and multilevel structures of biochars and their potential environmental applications: a critical review. Environ. Sci. Technol. 52 (9), 5027–5047.

Yang, H., Tong, M., Kim, H., 2012. Influence of bentonite particles on representative gram negative and gram positive bacterial deposition in porous media. Environ. Sci. Technol. 46 (21), 11627–11634.
Yang, X., Chen, Z., Wu, Q., Xu, M., 2018. Enhanced phenanthrene degradation in river sediments using a combination of biochar and nitrate. Sci. Total Environ. 619-620, 600–605.
Yuan, P., Wang, J., Pan, Y., Shen, B., Wu, C., 2019. Review of biochar for the management of contaminated soil: preparation, application and prospect. Sci. Total Environ. 659, 473–490.
Zhang, H., Tang, J., Wang, L., Liu, J., Gurav, R.G., Sun, K., 2016. A novel bioremediation strategy for petroleum hydrocarbon pollutants using salt tolerant *Corynebacterium variabile* HRJ4 and biochar.. J. Environ. Sci. 47, 7–13.
Zhao, L., Cao, X., Mašek, O., Zimmerman, A., 2013. Heterogeneity of biochar properties as a function of feedstock sources and production temperatures. J. Hazard. Mater. 256-257, 1–9.
Zhao, L., Xiao, D., Liu, Y., Xu, H., Nan, H., Li, D., et al., 2020. Biochar as simultaneous shelter, adsorbent, pH buffer, and substrate of *Pseudomonas citronellolis* to promote biodegradation of high concentrations of phenol in wastewater. Water Res. 172, 115494–115504.
Zhao, W., Zhao, P., Tian, Y., Shen, C., Li, Z., Jin, C., 2019. Transport and retention of *Microcystis aeruginosa* in porous media: impacts of ionic strength, flow rate, media size and pre-oxidization. Water Res. 162, 277–287.
Zhong, H., Liu, G., Jiang, Y., Yang, J., Liu, Y., Yang, X., et al., 2017. Transport of bacteria in porous media and its enhancement by surfactants for bioaugmentation: a review. Biotechnol. Adv. 35 (4), 490–504.